Vehicle System Dynamics

International Journal of Vehicle Mechanics and Mobility

ISSN: (Print) (Online) Journal homepage: https://www.tandfonline.com/loi/nvsd20

Adaptive stability mechanism of high-speed train employing parallel inerter yaw damper

Xiaoxia Zhang, Hu Li, Jun Cheng, Longjiang Sheng & Yuan Yao

VEHICLE SYSTEM DYNAMICS
2023, VOL. 61, NO. 1, 38–57
https://doi.org/10.1080/00423114.2022.2045027

Adaptive stability mechanism of high-speed train employing parallel inerter yaw damper

Xiaoxia Zhang[a,b], Hu Li[b], Jun Cheng[b], Longjiang Sheng[c] and Yuan Yao[b]

[a]School of Mechanical Engineering, Chengdu University of Technology, Chengdu, People's Republic of China; [b]State Key Laboratory of Traction Power, Southwest JiaoTong University, Chengdu, People's Republic of China; [c]Bogie R&D Department, CRRC Zhuzhou Electric Locomotive Co., Ltd., Zhuzhou, People's Republic of China

ABSTRACT

The aim of the study is to design a secondary yaw suspension that will control both low-frequency body motion and bogie hunting under different wheel–rail equivalent conicities. In order to enable the high-speed train to adaptively adjust to different wheel tread wear stages and improve the lateral dynamic performance of the vehicle in extreme wheel–rail contact states without any sensors and control systems, the eddy current damper with the parallel inerter as the yaw damper is proposed, and the in-depth research on its working mechanism is conducted. By establishing the theoretical analysis model of the lateral dynamics of high-speed train, and the multi-objective optimisation of the vehicle performances is carried out. The optimal parameters of the yaw damper under different wheel–rail contact conditions are analysed and the importance of frequency-dependent stiffness of yaw damper is obtained. Based on the characteristics of high-frequency transmissibility of inerter, the parallel inerter is applied to solve the limitation of insufficient dynamic stiffness of the traditional hydraulic yaw damper. The parameter configuration of the yaw damper with small series stiffness and large parallel inerter is proposed, and the stable operation of trains in major wheel–rail contact equivalent conicity is realised by using its frequency-dependent stiffness characteristics. In addition, the optimal energy dissipation and negative stiffness conditions of the parallel inerter yaw damper are analysed in this paper.

ARTICLE HISTORY
Received 27 May 2021
Revised 20 October 2021
Accepted 12 December 2021

KEYWORDS
High-speed train; adaptive stability; yaw damper; inerter; frequency-dependent stiffness; eddy current damper

1. Introduction

Suspension systems and reasonable parameter configurations are important measures to achieve desirable dynamic performances of high-speed trains, and the yaw damper is an important suspension element to ensure the hunting stability of wheel–rail vehicles. Due to the wear of the wheel–rail system and track grinding, the invariable parameter yaw damper is hard to compromise the requirements of vehicle stability in a large range of wheel–rail contact conditions. For high-speed trains, low-frequency body hunting can

CONTACT Yuan Yao yyuan8848@163.com

occur under the low wheel–rail conicity contact condition, which is called primary hunting or carbody hunting, while high-frequency bogie hunting occurs under extremely high wheel–rail conicity condition, which is called secondary hunting or bogie hunting. The insufficient stability or instability of both will deteriorate the lateral dynamic performance of vehicles. The aim is to design a secondary yaw suspension that will control both low-frequency body motion and bogie hunting under different wheel–rail equivalent conicities. Active suspension technology has been proposed and has achieved good results to meet this requirement [1–4]. However, due to the problems of high costs, numerous components and high requests for control technology in practical application, it has not been widely adopted in service operation. By making full use of the frequency-dependent stiffness characteristics to increase the dynamic stiffness amplitude of the yaw damper, the parameters can be adjusted according to the action frequency of the damper to achieve the adaptive stability of high-speed trains under different wheel–rail contact conditions. To solve this problem, this paper proposes a scheme of using the parallel inerter yaw damper for railway vehicles to automatically adapt to different wheel–rail contact states without any sensors and control systems. Using its frequency-dependent stiffness characteristics, the adaptive stability of high-speed trains in a large range of wheel–rail contact states is realised. The lateral dynamic performances of trains especially in extreme wheel–rail contact conditions are improved. The shape preservation requirements of the train for wheel tread and rail profile are reduced, thereby reducing the operation and maintenance costs.

Inerters have been widely studied and applied in civil engineering, ships, automobiles, machinery manufacturing and other engineering fields [5–7], and there are also corresponding studies on railway vehicles. In 2009, Wang et al. [8] proposed three inerter-spring-damper (ISD) theoretical models and discussed the dynamic performance of the ISD model installed on the rail vehicle. The riding quality index was improved after using the inerter, but the dynamic wheel load would deteriorate, and the high-order controller can further optimise its performance. In 2012, Jiang et al. [9] established a variety of passive suspension models considering the inerter and applied them to the simulation of railway vehicles. Compared with the vehicle model using the traditional damper, in some special cases, such as when the lateral stiffness of the primary system is large, replacing the traditional damper of the secondary system with the inerter can significantly improve the dynamic performance of the train, demonstrating the rationality of using the inerter as the vertical and lateral damper of the secondary system. Recent studies have shown that the use of inerter in primary suspension of railway vehicles can improve vehicle riding quality and wheel–rail wear performance simultaneously [10,11].

2. The frequency-dependent characteristics of the damper

An eddy current damper is a new type of damper, which realises structural vibration control by eddy current damping force generated by electromagnetic induction. Eddy current dampers have the advantages of strong linear damping characteristics and adjustable damping coefficient, which is easy to realise semi-active control. It has been widely used in the field of vibration control of aerospace structure and rotating mechanism. In recent years, it has been applied in structural vibration control engineering and other fields, and the application in ground vehicles has also begun to be studied [12]. The eddy current damper is composed of ball screw, permanent magnet, induction coil and outer cylinder.

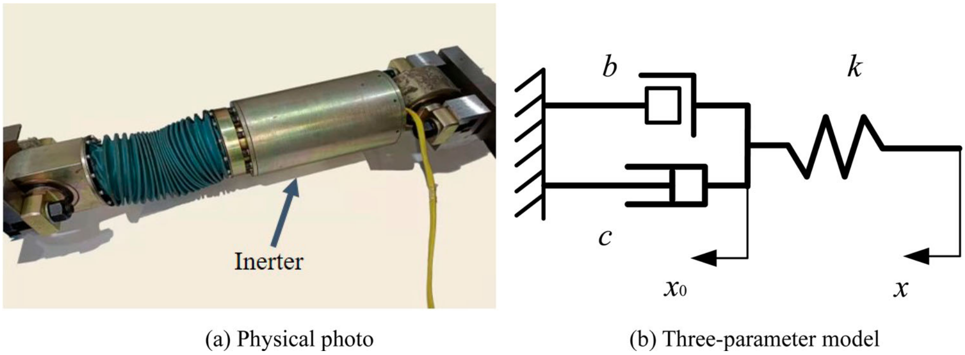

Figure 1. Parallel inerter yaw damper.

The physical photo is shown in Figure 1(a). In order to increase the eddy current damping force, the eddy current damper converts the axial motion into the rotational motion of the outer cylinder through the ball screw and improves the cutting magnetic field velocity of the coil on the outer cylinder. At the same time, the rotational inertia of the outer cylinder forms the inertia characteristics. The damper has damping with the parallel inerter. The inertance b is

$$b = J \cdot \left(\frac{2\pi}{P}\right)^2 \tag{1}$$

where J is the rotational inertia of inerter (kg m^2) and P is the ball screw pitch (m). When P is 10 mm and J is 0.026 kg.m^2, the inertance b can be 10,000 kg.

Considering the rubber joints at both ends of the damper, if the nonlinear factors such as mechanical friction and clearance are ignored, the damper is theoretically a mechanical model with damping and inerter in parallel and then in series with stiffness. The three-parameter model considering series stiffness k, parallel damping c and inertance b is established as shown in Figure 1(b). The mathematical model of the system reads

$$k(x_0 - x) + c\dot{x}_0 + b\ddot{x}_0 = 0 \tag{2}$$

where x and x_0 are the displacements at the end and middle of the model, respectively. According to Laplace transform, we can get

$$\frac{x_0}{x} = \frac{\dot{x}_0}{\dot{x}} = \frac{k}{bs^2 + cs + k} \tag{3}$$

In which $s = j\omega$, ω is the circular frequency and j is the imaginary unit. F is the force of damper and can be expressed as

$$F = c\dot{x}_0 + b\ddot{x}_0 = \frac{k(c + bs)}{bs^2 + cs + k}\dot{x} = \frac{k(cs + bs^2)}{bs^2 + cs + k}x \tag{4}$$

The equivalent stiffness k_e and equivalent damping c_e at both ends of the damper are

$$k_e = \frac{k(bs^2 + cs)}{bs^2 + cs + k} \tag{5}$$

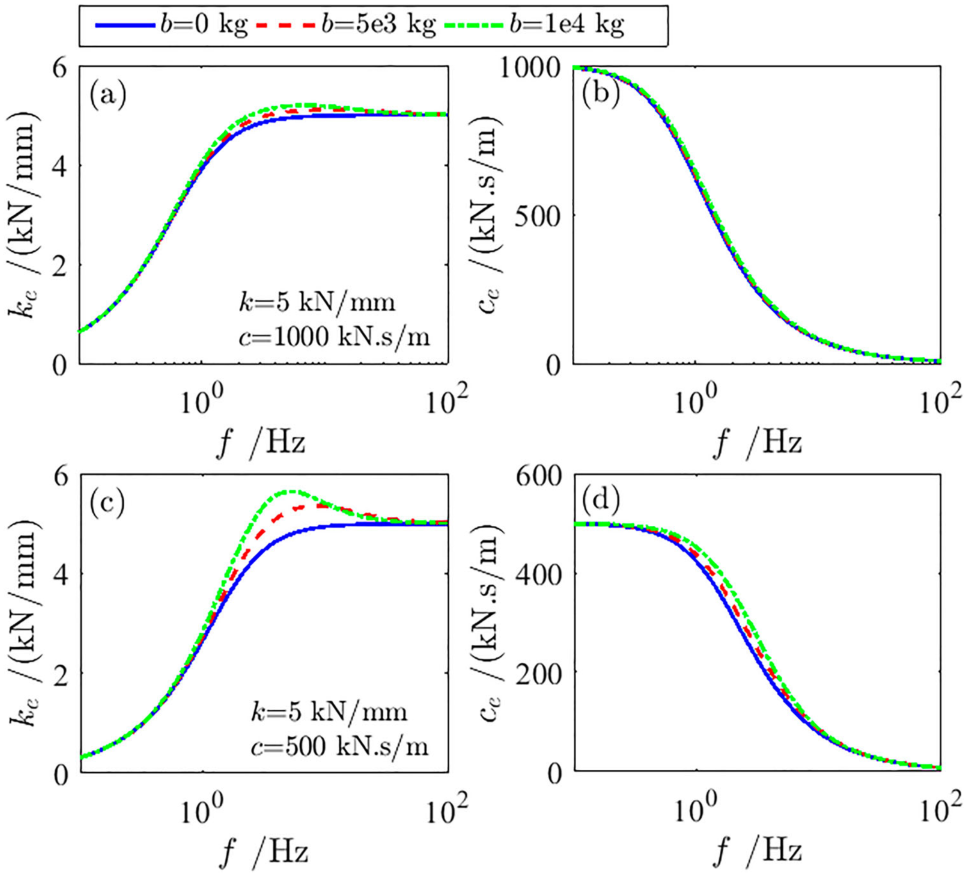

Figure 2. Frequency characteristics of the three-parameter model.

$$c_e = \frac{k(bs + c)}{bs^2 + cs + k} \tag{6}$$

It can be seen that the equivalent stiffness and equivalent damping are related to the action frequency of the two ends of damper, which is also known as dynamic stiffness and dynamic damping. The frequency-dependent characteristics are shown in Figure 2. At low frequency, the damper mainly reflects the damping characteristics and the stiffness of the damper can be ignored. With the increase of frequency, the stiffness characteristics of the damper increase; meanwhile, the damping characteristics decrease. When the frequency of the damper reaches a certain value, the sum of damping force and inertia force is large, and the relative displacement of the damper is mainly compensated by the series stiffness. The stiffness of the damper is close to the series stiffness value, and the damping and inertia effects are small. The parallel inerter increases the equivalent stiffness as well as the equivalent damping characteristic of the damper in the resonant range. When the damper damping c is small, the increased effect of equivalent stiffness and equivalent damping is more obvious. The parallel inerter enlargers the frequency-dependent stiffness and frequency-dependent damping features especially in resonance.

Substitute $s = j\omega$ into Equation (5) to get the complex stiffness k_e

$$k_e = (1 + j\eta)k^* \tag{7}$$

In Equation (7), the real part $k*$ and the imaginary part $\eta k*$ are called the storage modulus and energy dissipation modulus, respectively, which read

$$k^* = \frac{k[b^2\omega^4 + (c^2 - bk)\omega^2]}{(k - b\omega^2)^2 + c^2\omega^2} \tag{8}$$

$$\eta k^* = \frac{k^2 c\omega}{(k - b\omega^2)^2 + c^2\omega^2} \tag{9}$$

where η is the dissipation factor and $\phi = \tan^{-1}(\eta)$ is the dissipation angle. The storage modulus and energy dissipation modulus represent the ability of the damper storing energy and damping converting mechanical energy into thermal energy, respectively. With the increase of frequency, its stiffness increases, and the corresponding energy storage effect of the damper increases. The energy dissipation effect increases first and then decreases, that is, the damper has the optimal energy dissipation condition.

When the inertance $b = 0$, which is equivalent to the stiffness and damping series Maxwell model of conventional hydraulic damper. Make $\frac{d\eta k^*}{d\omega} = 0$, by calculating its maximum value, the optimal dissipation energy condition can be obtained as follows:

$$\omega_{opt} = \frac{k}{c} \tag{10}$$

For Equation (8) and Equation (9), when $(k{-}b\omega^2) = 0$, the resonance occurs, and the resonance frequency is $\omega_r = \sqrt{k/b}$.

For the three-parameter damper model, the damping force and inertia force are great at medium and high frequencies. Due to the opposite phase between acceleration and displacement, the inertia force makes the damper exhibit negative stiffness characteristics. According to Equation (8), if $b^2\omega^2 + c^2 - bk \leq 0$, that is, under the condition of $k \geq 2\omega c$, when b satisfies Equation (11), the damper appears negative stiffness or zero stiffness, as shown in Figure 3.

$$b \in \left[\frac{k - \sqrt{k^2 - 4\omega^2c^2}}{2\omega^2}, \frac{k + \sqrt{k^2 - 4\omega^2c^2}}{2\omega^2}\right] \tag{11}$$

If $c = 0$, when $k \geq b\omega^2$, the damper has negative stiffness or zero stiffness. The curves of storage modulus and energy dissipation modulus with different parameters b, k and c are shown in Figure 3.

3. Vehicle lateral dynamic performances

3.1. The vehicle linear dynamics model

In order to investigate the vehicle hunting stability, a simplified vehicle lateral dynamic model is established, as shown in Figure 4. The model is composed of 19 rigid bodies, which

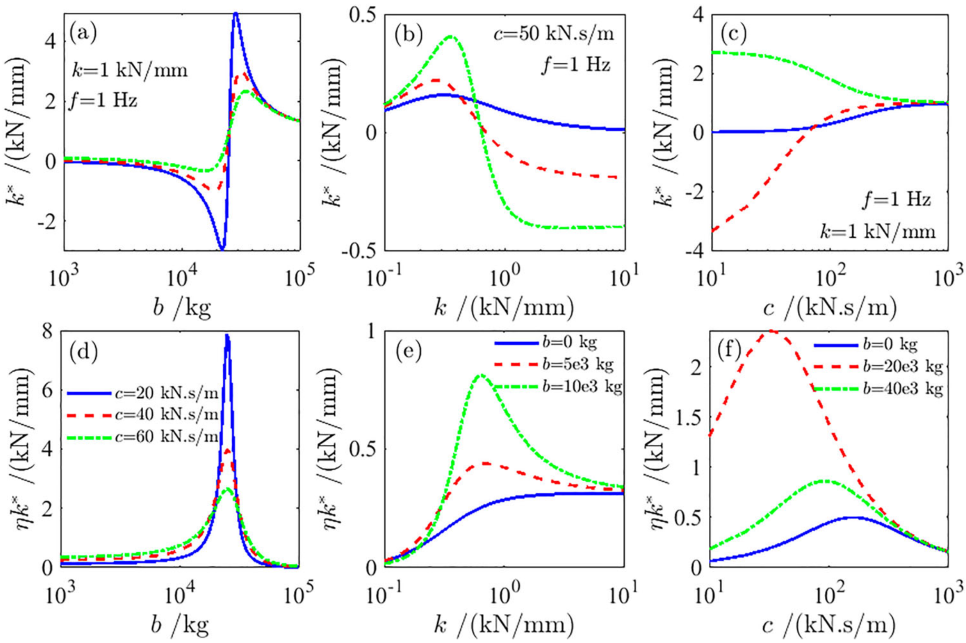

Figure 3. Parameter characteristics of the three-parameter model.

are one carbody, two frames, four motors, four wheelsets and eight damper virtual mass. The carbody and the frame have lateral, yaw and roll degrees of freedom, and the motors have lateral degrees of freedom. The wheelsets have lateral and yaw degrees of freedom. The virtual mass of the damper has one degree of freedom to realise the series stiffness. The primary suspension is between the wheelset and the frame, which is composed of lateral, longitudinal and vertical suspension stiffness. Besides, the rotating arm length of primary suspension is considered in the model. The secondary suspension is between the carbody and the frame, which is composed of lateral, longitudinal and vertical stiffness, damping and anti-roll stiffness. In order to analyse the effects of the parallel inerter damper on vehicle stability, the yaw damper is established based on the three-parameter model as shown in Figure 1(b). The secondary lateral damper is established based on the Maxwell model that consists of spring and damper in series. The dynamics model has 29 degrees of freedom. The linear stability of the established vehicle model is emphatically analysed in this study; thus, the wheel–rail contact geometry is expressed by equivalent conicity, and the wheel–rail tangential force is calculated by linear Kalker theory. Referring to one type of high-speed EMU (Electric Multiple Unit) in China [13,14], the specific parameters of the model are shown in Table 1. It adopts small yaw damping and large primary longitudinal stiffness, as well as elastic suspension of driving system. The equation of the system dynamics model is as follows:

$$M\ddot{x}(t) + C\dot{x}(t) + Kx(t) = Q \tag{12}$$

The $\boldsymbol{x}$ is the degree of freedom vector of the system. The matrices M, C, K and Q are the mass, damping, stiffness and external force components of the system, respectively. For the motion equation of a single wheelset with an elastic primary suspension, the lateral

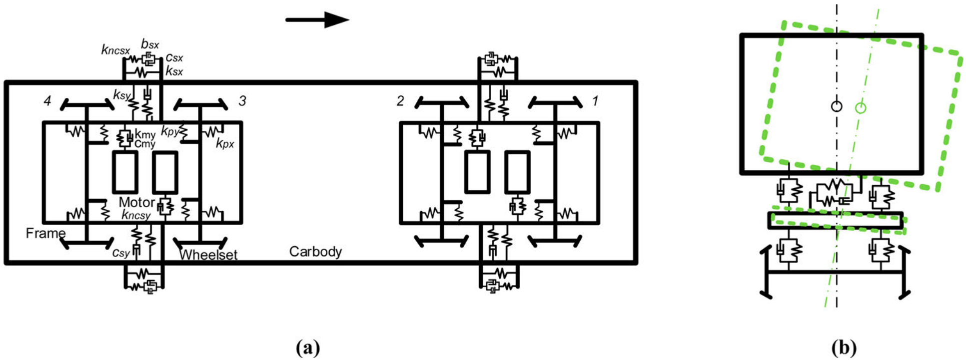

Figure 4. Simplified vehicle lateral dynamics model.

and yaw movements of the wheelset are coupled by the wheel–rail tangential forces. Due to the coupling effect of the inerter on the correlated mass, M is non-diagonal, as shown in Equation (13). K is an asymmetric stiffness matrix, and the non-diagonal items represent the coupling of the wheelset's lateral and yaw movement caused by the interaction of wheel and rail in tangential direction. The system damping C is related to the running speed v. In a period of hunting motion, if the input and the consumed energy are equal, the linear system is in the critical stability state. The corresponding speed v is the linear critical speed.

$$M = \begin{bmatrix} \ddots & & & & & \\ & I_f + bsx \cdot 2l_{cx}^2 & \cdots & -bsx \cdot l_{cx} & bsx \cdot l_{cx} & \\ & \vdots & \ddots & \vdots & \vdots & \\ & -bsx \cdot l_{cx} & \cdots & m_{cx} + bsx & 0 & \\ & bsx \cdot l_{cx} & \cdots & 0 & m_{cx} + bsx & \\ & & & & & \ddots \end{bmatrix} \tag{13}$$

Due to the unsymmetrical nature of the stiffness matrix K, Equation (12) cannot be transformed into an uncoupled set of differential equations by means of conventional methods of modal analysis, i.e. using only real modes. A solution can still be affected though by using the complex modal transformation. To do this, Equation (12) is recast into the following state-space form:

$$\dot{y}(t) = \mathrm{A}y(t) \tag{14}$$

The vector y is the system state vector, and the system matrix A is given by

$$A = \begin{bmatrix} 0_{29\times29} & I_{29\times29} \\ -M^{-1}K & -M^{-1}C \end{bmatrix} \tag{15}$$

The modal shapes and linear stability of the vehicle system are obtained by analysing the eigenvectors and eigenvalues of A.

Table 1. The vehicle model parameters.

Symbol	Definition	Value
m_w	Mass of the wheelset	1639 kg
I_w	Yaw inertia of the wheelset	822 kg.m^2
m_f	Mass of bogie frame	2328 kg
I_{fx}	Roll inertia of bogie frame	2110 kg.m^2
I_{fz}	Yaw inertia of bogie frame	4080 kg.m^2
m_c	Mass of carbody	38936 kg
I_{cx}	Roll inertia of carbody	1.67e6 kg.m^2
I_{cy}	Yaw inertia of carbody	9.61e5 kg.m^2
m_m	Mass of motor	750 kg
m_{cx}	Mass of yaw damper	20 kg
k_{pz}	Primary vertical stiffness per axle	0.75 kN/mm
k_{sx}	Secondary longitudinal stiffness	0.133 kN/mm
k_{sy}	Secondary lateral stiffness	0.133 kN/mm
k_{sz}	Secondary vertical stiffness	0.2 kN/mm
c_{sz}	Secondary vertical damper damping	10 kN s/m
c_{pz}	Primary vertical damper damping	10 kN s/m
$k\phi$	Stiffness of anti-roll torsion bar	4.15 MN m/rad
$2l_1$	Lateral spacing of primary suspension	2000 mm
l_b	Length of axle box arm	480 mm
$2b$	Wheel base	2500 mm
$2L$	Length between bogie centres	17375 mm
$2l_0$	Distance of the contact spot	1493 mm
$2l_2$	Lateral spacing of the secondary suspension	2200 mm
$2l_{cx}$	Lateral spacing of the yaw damper	2700 mm
r_0	The wheel rolling radius	460 mm
f_ξ	The longitudinal creep coefficient	1e7 N
f_η	The lateral creep coefficient	1e7 N
k_r	The contact stiffness of the wheel–rail	500 kN/mm
λ_e	Wheel–rail contact conicity	0.05, 0.17, 0.30
V	Running speed	350 km/h
k_{px}	Primary longitudinal stiffness per axle	120 kN/mm
k_{py}	Primary lateral stiffness per axle	12.5 kN/mm
c_{sy}	Secondary lateral damper damping	15 kN s/m
$kncsx$	Series stiffness of yaw damper damping	*Optimised*
csx	Yaw damper damping	*Optimised*
bsx	Parallel inerter of yaw damping	*Optimised*

3.2. Linear stability analysis

The vehicle dynamics model in Section 3.1 is used to calculate the eigenvalue of the system matrix A, and the ratio of the real part of the eigenvalue to the modulus of the eigenvalue corresponding to the hunting mode is solved, namely, the natural damping of the hunting mode, which is defined as the linear stability index ζ of the system. Usually, when the damping value is positive, it indicates that the linear system is stable. In this paper, the smaller value is selected as the optimisation direction, so we can define that the system is stable if ζ is negative.

In order to analyse the influence of series stiffness $kncsx$, damping csx and inertance bsx of the yaw damper on vehicle stability, the system linear stability index ζ corresponding to the combination of csx and $kncsx$ is calculated under different operating speeds v, equivalent conicities λ and inertances bsx. The results are shown in Figure 5. The horizontal axis is the variable $kncsx$ and the vertical axis is the variable csx. Each subgraph in the figure represents the contour of the linear stability index ζ. The deeper the colour is, the smaller the stability index is, and the better the vehicle lateral stability is. In the figure, the virtual

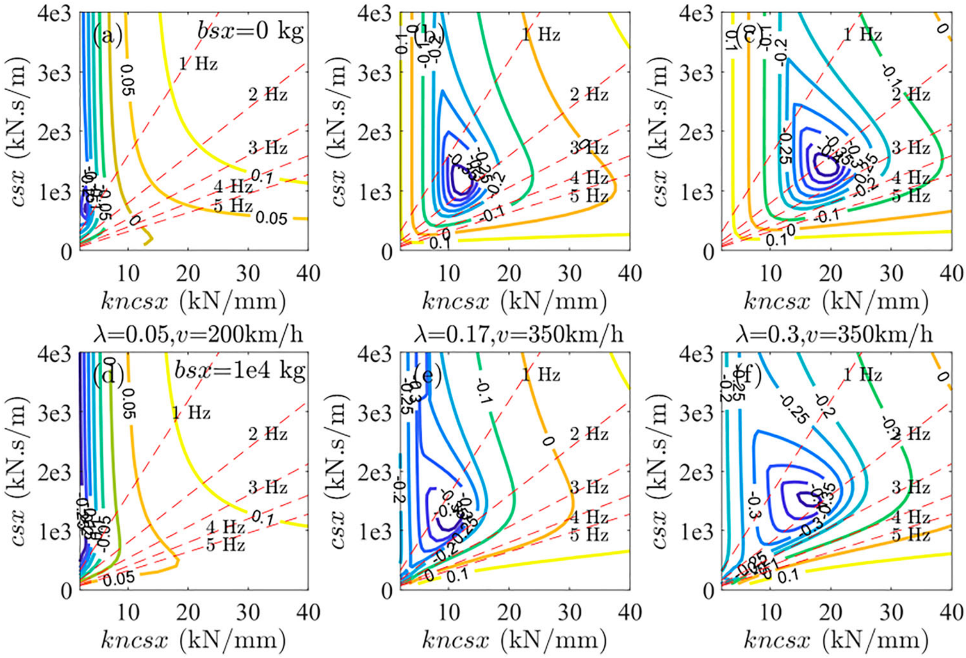

Figure 5. Linear stability of vehicle with different parameters of yaw damper.

line represents the parameter matching relationship between *csx* and *kncsx* when different action frequencies meet the optimal dissipation condition of Equation (10). In Figure 5, subgraphs (a), (b) and (c) are the results of using traditional hydraulic yaw damper with *bsx* of 0 kg. The equivalent conicity λ from left to right is 0.05, 0.17 and 0.3, respectively. Considering that low conicity is prone to hunting instability at low speed, the former calculation speed *v* is 200 km/h, and the latter two *v* is 350 km/h. It can be seen from the figure that with the increase of equivalent conicity, the series stiffness *kncsx* needs to be increased to improve the hunting stability of the vehicle. The optimal *csx* value is about 500–1500 kN s/m, and the optimal *csx* increases with the increase of equivalent conicity. The optimal parameters *kncsx* and *csx* of the yaw damper in the figure generally meet the optimal dissipation condition of Equation (10), that is, the ratio of optimal *kncsx* to *csx* is close to the circular frequency of hunting mode. The vehicle hunting frequency increases with λ and *v*, and the corresponding optimal ratio of *kncsx* to *csx* increases. In Figure 5, subgraphs (d)–(f) show the results with *bsx* of 1e4 kg. Compared with the non-inerter, the optimal *csx* is almost unchanged, but the optimal *kncsx* value decreases significantly in the high conicity conditions. In addition, the stability index of the system is also improved obviously in high conicity conditions when *kncsx* is smaller than the optimal value. For instance, the stability index can reach −0.3 in the subgraph (f) at *kncsx* of 10 kN/mm, but it is only −0.15 in the subgraph (c). It means that the vehicle stability will not deteriorate significantly in the state of wheel–rail extremely worn if the parallel inerter on the yaw damper has been equipped.

In short, the optimal series stiffness of the high-speed train yaw damper is related to the equivalent conicity of wheel–rail contact and the operating speed of the vehicle, namely the corresponding hunting frequency. The optimal series stiffness decreases with the decrease of hunting frequency, especially in the low wheel–rail contact conicity condition, a smaller series stiffness is required. However, a larger series stiffness of the yaw damper is required for high conicity. Due to the rubber joint stiffness of the yaw damper is fixed in practice, the variation range of damper dynamic stiffness under different frequencies is limited. The selection of yaw series stiffness needs to compromise the contradiction between high and low wheel–rail contact conicity for vehicle lateral stability, so it cannot guarantee vehicle stability in extreme wheel–rail contact conditions. The parallel inerter yaw damper adopts a small series stiffness to meet the low-frequency carbody huntiong stability. With the increase of the hunting frequency, the inerter at high frequency increases the stiffness characteristics of the yaw damper, which can still ensure the lateral stability of high-frequency bogie hunting. In addition, the greater the energy dissipation power of the damper is, the more stable the vehicle system is. The matching of series stiffness and damping can be realised based on the optimal dissipation theory, that is, the ratio of stiffness to damping is equal to the circular frequency of the vehicle hunting.

3.3. Frequency domain riding index

Riding quality is an important index to evaluate the performances of vehicle suspension system. The commonly used Sperling Index is as follows:

$$W = 0.896 \times \sqrt[10]{\sum_{i=1}^{n} {A_i}^3 \frac{F(f_i)}{f_i}} \tag{16}$$

In which A_i denotes the maximum value of acceleration vibration at frequency f_i (cm/s^2). f_i denotes the ith vibration frequency (Hz). $F(f_i)$ is the frequency weighting coefficient. The values of 2.5, 2.75 and 3.0 indicate the riding quality of excellent, good and acceptable rank, respectively.

The frequency domain method is an improvement of the Sperling Index. In the Sperling formula, the acceleration vibration value is replaced by the integration of the power spectrum function of acceleration time operation samples in the frequency range. The new formula is as follows:

$$W = C_1 \times \sqrt[6.67]{2\int_0^f G_1(f){B_1}^2 \, \mathrm{d}f} \tag{17}$$

in which $G_1(f)$ is the power spectral density function of acceleration ((m/s^2)^2/Hz), C_1 is 0.83 for the lateral riding quality calculation and B_1 is a frequency weighting function.

In this paper, the frequency response function of lateral vibration of carbody on the random track irregularity state is obtained by the pseudo-excitation method [15,16]. The frequency domain riding quality index calculation has the advantage of fast calculation because it does not need time domain simulation of the dynamics model, which is conducive to the multi-objective and multi parameter optimisation analysis of vehicle suspension parameters. The Wuhan–Guangzhou high-speed railway track lateral irregularity spectrum with the frequency range from 0.3 to30 Hz is used as the track input, and the pseudo displacement response and pseudo acceleration response of the vehicle lateral dynamic system are calculated according to the pseudo-excitation method, so as to obtain the lateral riding quality indexes W_f and W_b of the front and rear ends of the carbody.

4. Parameter optimisation of damper

4.1. Multi-objective optimisation

The main task of the vehicle suspension parameter optimisation design is to find a class of compromise suspension parameters, so that it can compromise the lateral stability, curve passing and riding quality of the train. However, the lateral stability is more important, and the curve passing performance for the high-speed train is the optimisation objective in this study due to the large radius of high-speed railway. For lateral stability, on the one hand, when the wheel–rail contact conicity is low, such as the state of new wheel and new rail profile, the lower hunting frequency is close to the natural vibration frequency of the carbody suspension, so the carbody is prone to a hunting motion or called primary hunting. Primary hunting is characterised by low-frequency lateral sway of the carbody and mainly affects the ride comfort. On the other hand, the high wheel–rail equivalent conicity after wheel tread wear makes the stability margin of the bogie hunting insufficient, and the secondary hunting or called bogie hunting occurs, which is manifested as the high-frequency lateral shaking of the bogie. To describe the lateral stability of trains under two different wheel–rail contact conditions, the low conicity stability index ζ_{low} corresponding to wheel–rail contact conicity λ of 0.05 and the high conicity stability index ζ_{high} corresponding to wheel–rail contact conicity λ of 0.3 are defined, respectively. The frequency domain lateral riding quality indexes Wy_{low} and Wy_{high} relative to the corresponding operating conditions are calculated, respectively, which take the larger values of the lateral riding quality of the front and rear ends of the carbody under the corresponding wheel–rail contact conditions. When the value of ζ is negative, it indicates that the system is stable, and the smaller the value is, the greater the hunting damping ratio under the wheel–rail contact condition is, and better the lateral stability is. Similarly, the smaller the riding quality index is, the better the vehicle lateral riding quality is. Vehicle lateral riding quality is related to lateral stability, especially in the low conicity condition. Existing studies have found that there is a contradictory relationship between the optimisation of ζ_{low} and ζ_{high} for the selection of some parameters, that is, the better the low conicity stability of the vehicle is, the worse the high conicity stability is and vice versa [13,14]. Therefore, the lateral stability optimisation design of bogie suspension parameters is a multi-objective optimisation process.

Multi-objective optimisation problems usually have a solution set, which is called Pareto solution, and its image in the objective function space is called Pareto frontier. The Pareto frontier is the objective values after optimisation; each point has the advantages that other points do not have, from which we can find the contradiction between the multiple objectives. According to the different design priorities, we can manually select the optimal solution to meet the performance requirements in the Pareto set. NSGA (Non-dominated Sorting Genetic Algorithm)-II algorithm [17] can keep the population diversity and improve computational efficiency. Thus, it is an effective algorithm for solving multi-objective optimisation problems. A fast non-dominated sorting genetic algorithm NSGA-II with the elitist strategy is selected for multi-objective optimisation design in this study. The yaw damper series stiffness *kncsx*, damping *csx* and parallel inertance *bsx* are taken as the optimisation parameters, and the parameter optimisation ranges of the three variables are from 5 to 20 kN/mm, 100 to 4000 kN s/m and 0 to 10,000 kg, respectively. The lateral riding quality indexes $Wy_{\_low}$ and $Wy_{\_high}$ corresponding to the high and low equivalent conicity conditions, and the low conicity stability index ζ_{low} are taken as the optimisation objectives. This multi-objective optimisation problem is stated as

$$\min \{Wy_{\_low},\ Wy_{\_high}, z_{low}\} \tag{18}$$

4.2. Multi-objective optimal results

The genetic algorithm NSGA-II is used to solve the multi-objective optimisation of vehicle dynamic performances for the three-parameter of the yaw damper. The Pareto frontier and Pareto parameter sets are obtained by iteration and updating the suspension parameters to optimise the vehicle system performances. To investigate the influence of yaw damper parameters on vehicle lateral stability, four hypothetical cases are considered, such as whether the inerter is contained and assuming that the damping and stiffness values in the three-parameter model are infinite. For the Maxwell model, if the stiffness is infinite, the yaw damper can be regarded as a pure damping force element. Similarly, if the damping is infinite, it can be regarded as a pure stiffness force element. Figure 6 is the Pareto frontier of optimisation objectives, which represents the best dynamic performance indexes of the vehicle under the defined calculation conditions. The horizontal axis and vertical axis in the figure are the riding quality indexes $Wy_{\_low}$ and $Wy_{\_high}$ corresponding to the high and low conicity conditions of the vehicle system, and the colour represents the vehicle low conicity stability index ζ_{low}. The smaller the ζ_{low} value is, the darker the colour in figure is. Designers can artificially select vehicle performance requirements from Pareto frontier and then obtain the corresponding optimisation parameters from Pareto sets.

In Figure 6, subgraph (a) shows collaborative optimisation of three parameters. Subgraph (b) is the case of the damper model without the inerter. Subgraph (c) and subgraph (d) show the pure stiffness and pure damping of damper with inerter, respectively. When considering collaborative optimisation of three parameters, the lateral riding quality index of vehicle can reach about 1.8 under the two conicity conditions; however, the lateral riding quality of the vehicle becomes worse without considering inerter. Subgraph (b) reflects the contradiction of vehicle lateral dynamic performances in the condition of high and low wheel–rail contact conicity. When ζ_{low} is less than −0.1, $Wy_{\_high}$ is greater than 2.6, which is unacceptable for the high-speed train. Subgraph (c) and subgraph (d) are pure stiffness and pure damping model of the damper containing inerter. The lateral riding quality of the vehicle with pure stiffness of the yaw damper is significantly better than that with pure damping. It shows that the mechanism of the yaw damper is not only the energy dissipation but also the stiffness characteristics to realise the yaw motion or hunting coupling between carbody and bogie.

Figure 7 shows the Pareto sets obtained by multi-objective optimisation, reflecting the relationship between optimisation parameters and optimisation objectives. The horizontal axis of each subgraph is the low conicity riding quality index $Wy_{\_low}$, and the vertical axis is the series stiffness *kncsx*, damping *csx* and inertance *bsx* of the yaw damper, respectively. For the collaborative optimisation of the three-parameter model as well as the pure stiffness

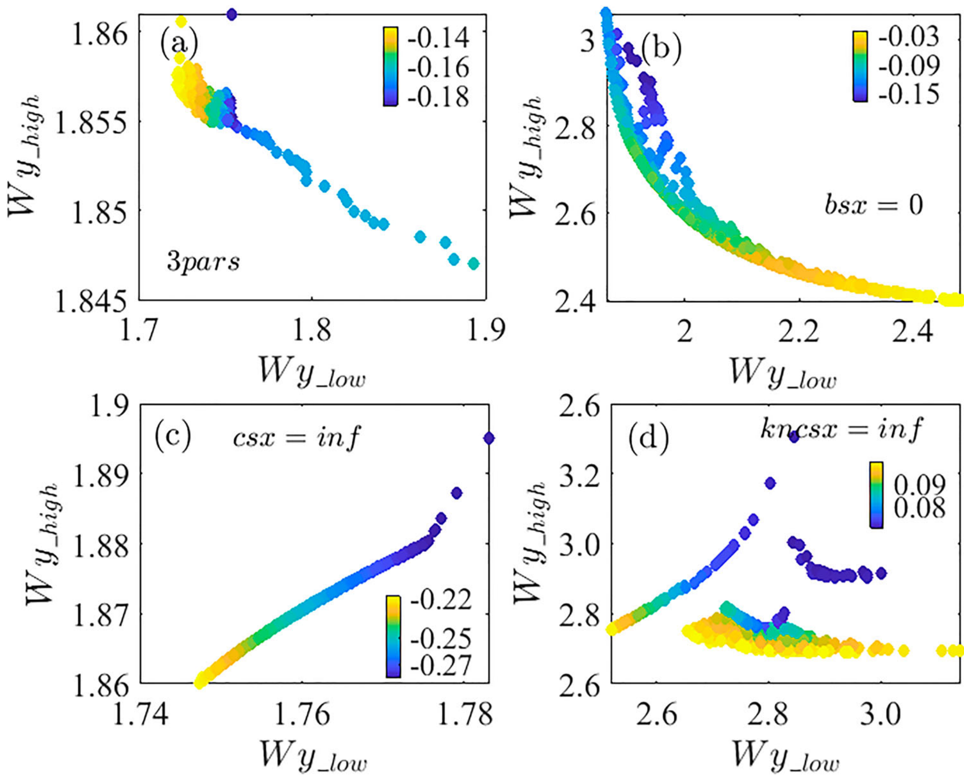

Figure 6. Multi-objective optimal results with different yaw damper models.

model with *csx* of infinity, the vehicle can achieve excellent lateral riding quality in the low conicity condition, which requires a small *kncsx* and a large *bsx*. If the inerter is not considered, the lateral riding quality is poor, and the optimal value of *csx* is 1000–2000 kN s/m. With the improvement of the low conicity riding quality $Wy_{\_low}$, *kncsx* needs to be reduced, as shown in the subgraph (a). If the yaw damper is a pure damping element with inerter, the lateral riding quality indexes in high and low conicity conditions that can be realised with any other *csx* and *bsx* are worse, and the optimal *csx* and *bsx* are both set to 0. Therefore, the above analysis results are verified. The stiffness characteristics of yaw damper are more important to realise the motion coupling between carbody and bogie. When the wheel–rail contact conicity is low, the stiffness of yaw damper needs to be reduced; conversely, it needs to be enlarged in the high conicity condition. The parallel inerter can enlarge the damper stiffness and realise yaw motion coupling between the carbody and the bogie at high frequencies, to achieve better lateral dynamic performances in high-speed and high wheel–rail contact conicity conditions.

4.3. Parameters optimisation configuration

For the yaw damper with the parallel inerter, it can be seen from the multi-objective optimisation of three parameters considering the lateral dynamic performances in high and low wheel–rail contact conicity conditions that the series stiffness *kncsx* of the yaw

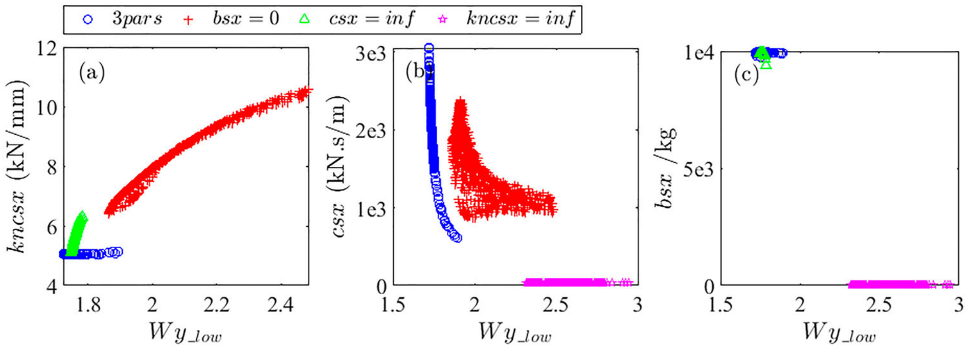

Figure 7. Optimal parameter sets with different yaw damper models.

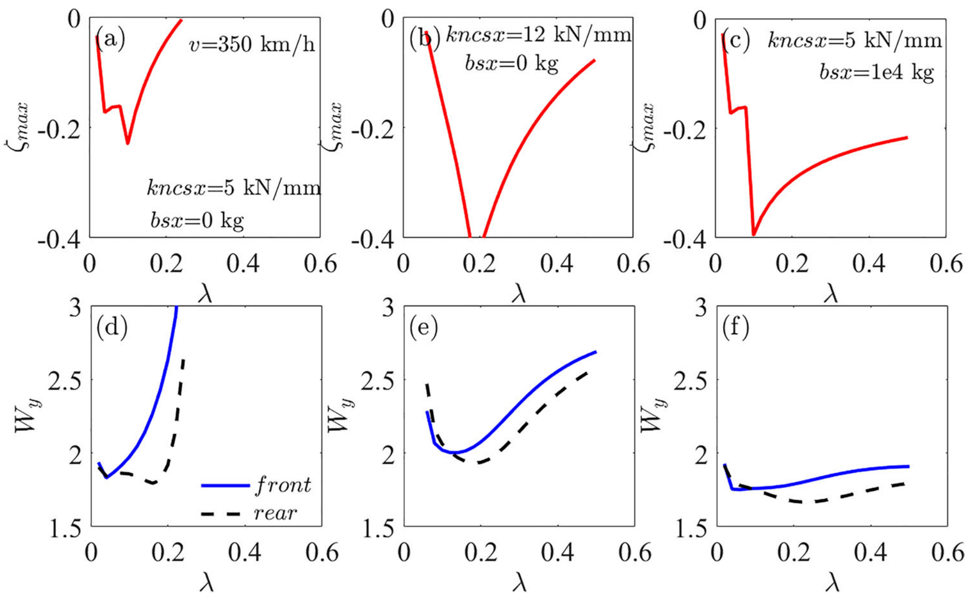

Figure 8. Influence of damper parameters on vehicle lateral dynamic performances.

damper should be selected to be smaller in the range of optimisation parameters, while the inertance *bsx* should be selected to be larger. For this type of high-speed train, the yaw damping *csx* is about 1000 kN s/m. In this section, several combination configurations of yaw damper parameters are selected to compare the lateral dynamic performances of the vehicle. In the first configuration, *kncsx* is 5 kN/mm and *bsx* is 0 kg. In the second configuration, *kncsx* is 12 kN/mm and *bsx* is 0 kg. In the third configuration, *kncsx* is 5 kN/mm and *bsx* is 10,000 kg. The first and second configurations, respectively, adopt a small and a large series stiffness value based on the traditional yaw damper without inerter. The third is that the yaw damper with the parallel inerter adopts a small series stiffness value. According to the actual high-speed train operation in China, the equivalent conicity from 0.02 to 0.5 is taken into account. The calculation results of vehicle lateral stability index ζ_{max} and carbody lateral riding quality index *Wy* at the speed of 350 km/h are shown in Figure 8.

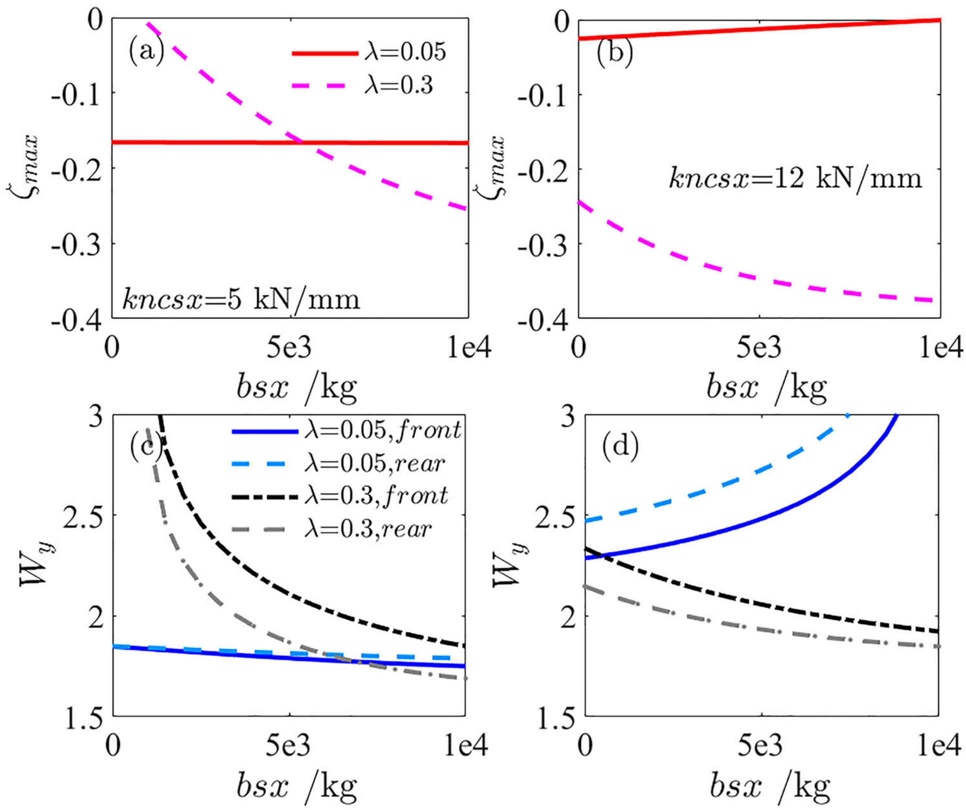

Figure 9. Influence of damper inerter on vehicle lateral dynamic performances.

For the first configuration, the yaw damper without inerter adopts a small series stiffness, and the vehicle has good lateral stability and lateral riding quality at the front and rear ends of carbody in the low conicity condition. However, the lateral dynamic performances are poor in the high conicity condition. In the second configuration, the opposite is true. That is, the traditional yaw damper without the inerter cannot give consideration to the vehicle stability in a wide range of wheel–rail contact conicity. In Figure 8, subgraph (c) and subgraph (f) show the calculation results of lateral stability and riding quality of the vehicle equipped with the parallel inerter yaw damper matching a small series stiffness in the third configuration, which can achieve excellent lateral dynamic performances both in low and high conicity conditions. It shows that the yaw damper with the parallel inerter has a positive effect on solving the contradiction of vehicle lateral dynamic performances in different wheel–rail contact conditions.

Figure 9 shows the influence of the parallel inertance *bsx* on the lateral dynamic performances of the vehicle with two series stiffness and two equivalent conicity values. It can be seen that the lateral dynamic performances are significantly improved with the increase of *bsx*, especially in the condition of small *kncsx* and high wheel–rail contact conicity. If using a large *kncsx*, the stability of the vehicle is poor in the low conicity condition, and the vehicle lateral dynamic performances deteriorate with the increase of *bsx*.

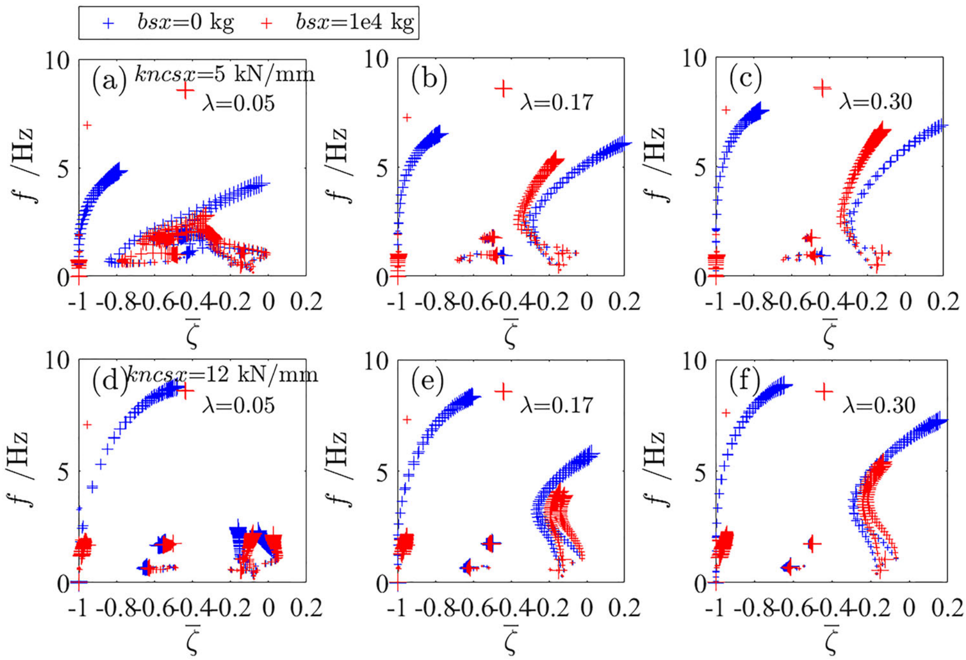

Figure 10. Root loci of vehicle at different speeds.

5. Root locus and modal energy analysis of system

In order to further study the mechanism of the yaw damper on high-speed trains, the root locus and hunting modal energy of vehicle dynamics model are analysed. The root loci of the vehicle linear system with the change of running speed corresponding to different wheel–rail contact equivalent conicity λ, yaw damper series stiffness *kncsx* and inertance *bsx* are shown in Figure 10. Each '+' represents the vibration frequency and modal damping ratio of a vibration mode at a certain speed. The larger '+' represents a larger running speed, and the velocity range is 20–800 km/h. The horizontal axis indicates the mode damping ratio $\overline{\zeta}$, which is the ratio of the real part of eigenvalues of the system matrix to the modulus of eigenvalues. It indicates the stable condition when the $\overline{\zeta}$ is less than 0. The less the $\overline{\zeta}$ is, the more stable the hunting motion of the vehicle is. When the $\overline{\zeta}$ is greater than 0, hunting instability will occur in the vehicle linear system model. The vertical axis indicates the modal frequency *f*, which is the imaginary part of eigenvalues. The root loci of vibration modes related to vehicle hunting within the frequency range of less than 10 Hz are mainly analysed. For this type of high-speed train, the lateral stability of the vehicle is determined by a single hunting root locus curve similar to the letter 'C' shape. Under the conditions of low speed and high speed, the stability of the low-frequency carbody hunting and the high-frequency bogie hunting is poor, respectively. Instead, the hunting stability is better in the middle speed range. The stability of this type of vehicle is determined by the hunting mode of the single root locus curve. That is, when the speed or the equivalent conicity of wheel–rail contact increases, the critical instability mode of the vehicle gradually evolves from the low-frequency carbody hunting to the high-frequency bogie hunting, and there is no hunting frequency transition, which

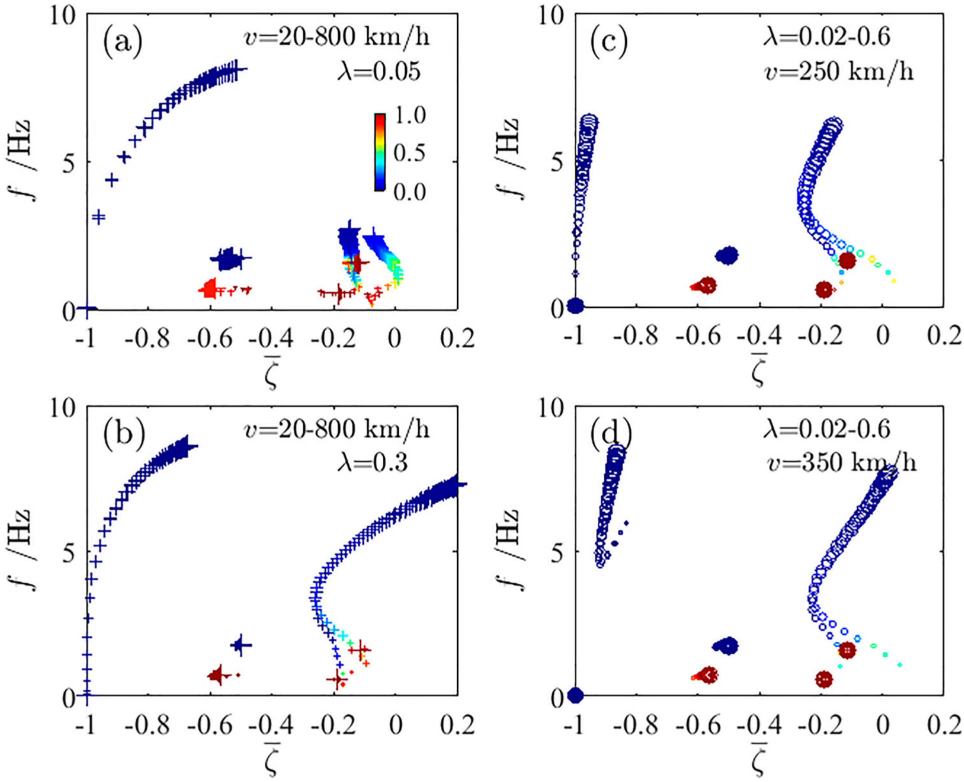

Figure 11. Modal energy distribution of vehicle body and bogie.

corresponds to the supercritical bifurcation characteristics in vehicle nonlinear dynamics. When *bsx* is 0, reducing *kncsx* is conducive to improving the low-frequency carbody hunting stability, while increasing *kncsx* is conducive to improving the high-frequency bogie hunting stability. When the *bsx* equals 10,000 kg, a small matching *kncsx* can achieve better low-frequency and high-frequency lateral hunting stability.

The vehicle hunting frequency increases with the increase of the running speed and the equivalent conicity of wheel–rail contact, and its lateral stability is poor in the low-frequency and high-frequency domains. The mechanism is explained according to the modal energy analysis of vehicle hunting. The hunting energy of the carbody and bogie under different operating speeds and equivalent conicity conditions is shown in Figure 11. The dark red in the figure indicates that the hunting energy of the carbody accounts for 100%. On the contrary, the blue part indicates that the hunting energy of bogie is relatively high. If the hunting frequency is close to the natural vibration frequency of carbody suspension, the hunting energy of carbody is large, and the carbody hunting stability is easy to deteriorate, which is called carbody or primary hunting instability. With the increase of hunting frequency, vehicle stability is improved but then becomes worse again. When the hunting frequency increases to a certain extent, high-frequency hunting instability occurs, which is called bogie or secondary hunting instability. The primary hunting is mainly carbody hunting motion, while the secondary hunting is mainly bogie hunting motion. In fact, if the stability is poor or instability occurs, the former is the low-frequency carbody

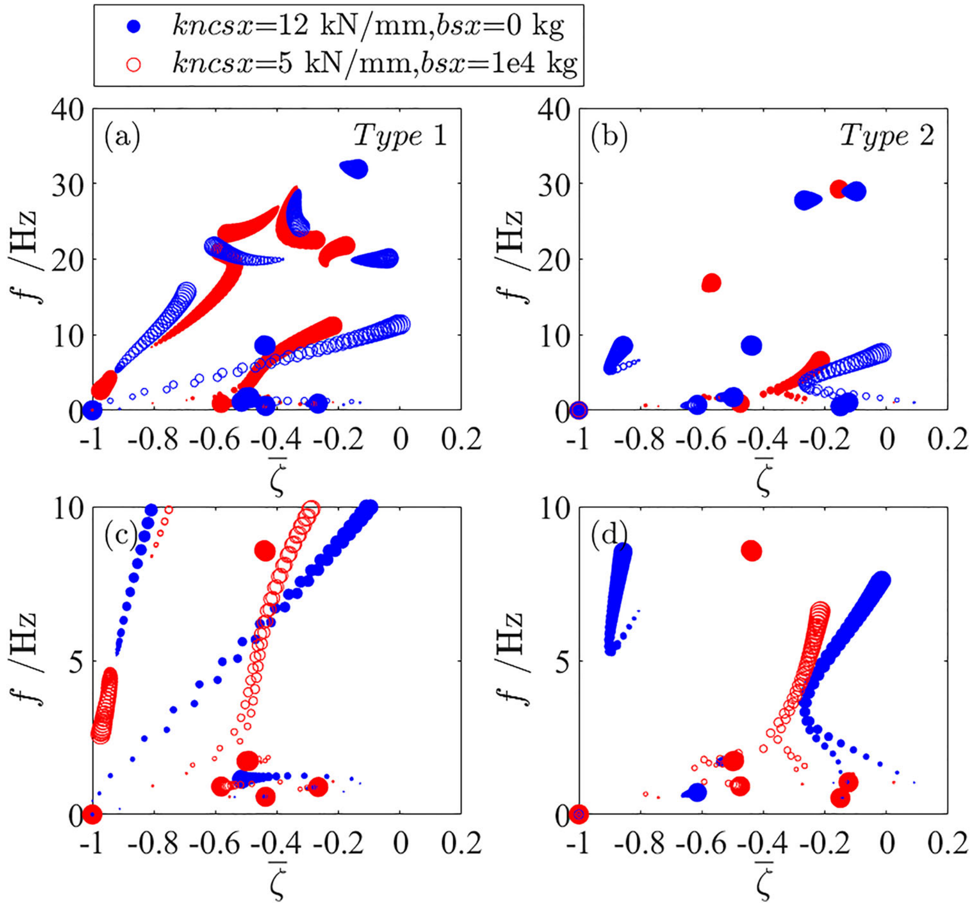

Figure 12. Root loci of vehicle under different equivalent conicities.

'sway' phenomenon, which leads to deterioration of ride comfort. Comparatively, the latter is the high-frequency bogie 'shaking' phenomenon, which reflects as the alarm accident of lateral acceleration of bogie frame.

According to the hunting energy proportion of vehicle in different frequency ranges, as well as the parameters optimisation law of the yaw damper, the stiffness action mechanism of the yaw damper for high-speed trains can be summarised. If the equivalent conicity of wheel–rail contact is low, the carbody hunting is the main proportion, and a smaller stiffness of yaw damper reduces the motion coupling between carbody and bogie, which is conducive to the stability of bogie hunting. When the equivalent conicity is high, the bogie hunting is the main energy, and the stiffness function of the yaw damper is conducive to suppressing the bogie hunting through the relatively static carbody. The hunting energy of bogie increases with the increase of equivalent conicity, and the corresponding optimal stiffness of the yaw damper needs to be increased.

In order to compare the application effects of the yaw damper with the parallel inerter on a variety of high-speed trains, the yaw damper adopts the optimisation configuration of *kncsx* and *bsx* in Section 4.3. The system stability of two types of high-speed trains in the literature [13] in different wheel–rail contact conicity conditions is investigated, and the vehicle discussed above is *Type* 2. The root loci of the two types of vehicles with wheel–rail contact equivalent conicity from 0.02 to 0.6 are drawn as shown in Figure 12. A larger circle symbol in the figure represents a larger equivalent conicity λ. The eigenvalue of vibration modes related to vehicle hunting within the frequency range of less than 10 Hz is mainly analysed, as shown in Figure 12(c,d). It can be seen from the comparison that the yaw damper with the parallel inerter can significantly improve the vehicle lateral stability, especially in the extreme wheel–rail contact conicity states, with which the risk of low-frequency carbody sways and high-frequency bogie shaking can be reduced significantly.

6. Conclusion

(1) In addition to the damping of yaw damper dissipating the vehicle hunting energy, the stiffness characteristic of the yaw damper is more critical to vehicle hunting stability. When the new wheel tread matches the newly grinding rail, the wheel–rail contact equivalent conicity is small, namely the low conicity condition, and the carbody hunting at a lower frequency is prone to take place, which leads to the carbody swaying phenomenon with a larger lateral amplitude. A smaller stiffness of the yaw damper is conducive to improving the carbody hunting stability. On the contrary, a larger stiffness of the yaw damper improves the coupling between carbody and bogie yaw motion, which is beneficial to suppress the high-frequency bogie hunting and improve the bogie hunting stability to reduce the risk of bogie high-frequency shaking.

(2) The eddy current damper converts reciprocal motion into rotational motion of the outer cylinder through the ball screw to improve the eddy current damping. The rotational outer cylinder acts as a inerter, which can realise high-frequency stiffness hardening of the damper. The frequency-dependent stiffness characteristics of the traditional hydraulic damper are not sufficient to meet the optimal stiffness requirements of high-speed trains in different wheel–rail contact conditions. The compromised stiffness parameters cannot realise the comprehensive optimisation of the dynamic performances of the vehicle in wide operating conditions, especially in extreme wheel–rail contact states. The frequency-dependent stiffness of the yaw damper with the parallel inerter can effectively solve this contradiction.

(3) A small radial stiffness of the rubber joint at both ends of the damper is suitable for the low-frequency primary hunting stability. Meanwhile, the parallel inerter can achieve the high stiffness requirements of the yaw damper in high-frequency conditions. The action frequency of the yaw damper varies with the train speed and wheel–rail equivalent conicity. The frequency-dependent stiffness of the yaw damper is adaptively adjusted to reduce the influence of the wheel–rail relationship such as equivalent conicity on vehicle stability, so as to realise the stable operation of trains in wide wheel–rail contact states. Therefore, the application of yaw damper with parallel inerter has a positive effect in improving the vehicle lateral stability in an abnormal wheel–rail contact condition adaptively, thus reducing the maintenance cost of high-speed trains as well as tracks.

Disclosure statement

No potential conflict of interest was reported by the author(s).

Funding

The material in this paper is based on work supported by National Science and Technology Support Program grant number (2018YFB1201703), National Natural Science Foundation of China (51735012), National Railway Group Science and Technology Program grant (N2020J028, N2020J026), and Traction Power State Key Laboratory grant (2022TPL_Q02) of the Independent Research and Development Projects.

References

[1] Yao Y, Wu G, Sardahi Y, et al. Hunting stability analysis of high-speed train bogie under the frame lateral vibration active control. Veh Syst Dyn. 2018;56(2):297–318.
[2] Yao Y, Li G, Sardahi Y, et al. Stability enhancement of a high-speed train bogie using active mass inertial actuators. Veh Syst Dyn. 2019;57(3):389–407.
[3] Zhang X, Wu G, Li G, et al. Actuator optimal placement studies of high-speed power bogie for active hunting stability. Veh Syst Dyn. 2020;58(1):108–122.
[4] Wei X, Zhu M, Jia L. A semi-active control suspension system for railway vehicles with magnetorheological fluid dampers. Veh Syst Dyn. 2016;54(7):982–1003.
[5] Lazar I, Neild S, Wagg D. Using an inerter-based device for structural vibration suppression. Earthq Eng Struct Dyn. 2014;43(8):1129–1147.
[6] Zan H, Wen H, Pan C, et al. The study of dynamic property analysis of the two-stage vibration isolation system for inerter. Mach Des Res. 2015;31(3):17–21. 26.
[7] Sun X, Chen L, Wang S, et al. Performance investigation of vehicle suspension system with nonlinear ball-screw inerter. Int J Automot Technol. 2016;17(3):399–408.
[8] Wang F, Liao M, Liao B, et al. The performance improvements of train suspension systems with mechanical networks employing inerters. Veh Syst Dyn. 2009;47(7):805–830.
[9] Jiang J, Matamoros-Sanchez AZ, Goodall RM. Passive suspensions incorporating inerters for railway vehicles. Veh Syst Dyn. 2012;50(suppl. 1):263–276.
[10] Jiang J, Matamoros A, Zolotas A, et al. Passive suspensions for ride quality improvement of two-axle railway vehicles. Proc Inst Mech Eng F J Rail Rapid Transit. 2015;229(3):315–329.
[11] Lewis T, Jiang J, Neild S, et al. Using an inerter-based suspension to improve both passenger comfort and track wear in railway vehicles. Veh Syst Dyn. 2020;58(3):472–493.
[12] Zhang H, Chen Z, Hua X, et al. Design and dynamic characterization of a large-scale eddy current damper with enhanced performance for vibration control. Mech Syst Signal Proc. 2020;145(11). doi:10.1016/j.ymssp.2020.106879.
[13] Yao Y, Li G, Wu G S, et al. Suspension parameters optimum of high-speed train bogie for hunting stability robustness. Int. J. Rail Transp. 2020;8(3):195–214.
[14] Chen X, Yao Y, Shen L, et al. Multi-objective optimization of high-speed train suspension parameters for improving hunting stability. Int. J. Rail Transp. 2021. doi:10.1080/23248378.2021.1904444
[15] Lin J. Virtual excitation method of random vibration. Beijing: Science Press; 2004.
[16] Liu X, Zhang Y, Guo H, et al. Random vibration analysis procedure of railway vehicle. Veh Syst Dyn. 2019;58(12):1873–1892.
[17] Deb K, Pratap A, Agarwal S, et al. A fast and elitist multiobjective genetic algorithm: NSGA-II. IEEE Trans Evol Comput. 2002;6(2):182–197.